IEEE Access
Multidisciplinary | Rapid Review | Open Access Journal

Received September 23, 2020, accepted September 29, 2020, date of publication October 7, 2020, date of current version October 21, 2020.

Digital Object Identifier 10.1109/ACCESS.2020.3029269

Delayless Block Individual-Weighting-Factors Sign Subband Adaptive Filters With an Improved Band-Dependent Variable Step-Size

JUNG-HEE KIM, (Member, IEEE), JEONG-HWAN CHOI, (Student Member, IEEE), SANG WON NAM, (Senior Member, IEEE), AND JOON-HYUK CHANG, (Senior Member, IEEE)
Department of Electronic Engineering, Hanyang University, Seoul 04763, South Korea

Corresponding author: Joon-Hyuk Chang (jchang@hanyang.ac.kr)

This work was supported in part by the Institute of Information and Communications Technology Planning and Evaluation (IITP) funded by the Korea Government (MSIT) (Intelligent Signal Processing for AI Speaker Voice Guardian) under Grant 2017-0-00474, and in part by the Institute of Information and Communications Technology Planning and Evaluation (IITP) funded by the Korea Government (MSIT) (Artificial Intelligence Graduate School Program, Hanyang University) under Grant 2020-0-01373.

ABSTRACT Delayless individual-weighting-factors sign subband adaptive filter (IWF-SSAF) algorithms with a band-dependent variable step-size (BDVSS) were recently introduced to achieve a robust convergence performance against the impulsive interference and to avoid an undesirable signal path delay in subband systems. In this paper, we develop a block implementation of the delayless IWF-SSAF algorithm designed for an active impulsive noise control (AINC) system. With the block-processing approach, the proposed delayless block IWF-SSAF algorithm can be implemented more efficiently than the original delayless algorithm regardless of number of subbands, which is verified through the computational analysis. Furthermore, an improved BDVSS version (I-BDVSS) is also proposed by using the multiple auxiliary past gradients, which are given for each band by the block-processing. Finally, the simulation results illustrate that the proposed delayless block IWF-SSAF algorithm with the I-BDVSS, even requiring less computational burden, can achieve a better convergence performance than the original delayless algorithm with the BDVSS under severe impulsive noise control environment.

INDEX TERMS Delayless structure, individual-weighting-factors sign subband adaptive filter, block implementation, active impulsive noise control, band-dependent variable step-size.

I. INTRODUCTION

Adaptive filter (AF) algorithms have been utilized in numerous applications such as system identification, signal prediction, and array processing [1]–[8]. Some applications such as acoustic echo cancellation (AEC) and wideband active noise control (ANC), demand very long AF with high computational complexity, which restricts its use in small and low-cost audio devices, e.g., earbuds. In addition, the AF with many taps also suffers from slow convergence for highly correlated signals. Subband AF (SAF) has received much attention for low computational complexity and fast convergence, whereby whitening signals are processed with lower order subfilters at a lower decimated sampling rate.

The associate editor coordinating the review of this manuscript and approving it for publication was Yingsong Li.

However, traditional SAF techniques accompany undesirable band-edge and aliasing effects [8]. As an attractive approach to addressing both issues, a novel SAF algorithm, called a normalized SAF (NSAF), was introduced by employing subband input signals without decimation into fullband weight update to alleviate the aliasing effect and by using a critically sampled structure to mitigate the band-edge effect [9]–[11]. The NSAF yields faster convergence than the normalized least-mean-square (NLMS) algorithm, but requires almost the same number of multiplications.

Several variants of the NSAF have been proposed under different backgrounds. Firstly, when impulsive interference occurs, the performance of the NSAF can be seriously deteriorated due to its ℓ_2-norm based nature. To resolve the problem, a sign SAF (SSAF) was introduced by incorporating a ℓ_1-norm based minimization into the NSAF

structure [12]. Furthermore, the convergence performance of the SSAF can be enhanced by adopting various variable step-size (VSS) schemes [13]–[17], and by fully utilizing the decorrelating property of the SSAF which leads to an individual-weighting-factors SSAF (IWF-SSAF) [18]. In addition to the SSAF based algorithms, several M-estimate based NSAF algorithms and their variable step-size (VSS) schemes have been also presented to improve the robustness of the NSAF against the impulsive noise [19], [20]. Secondly, the NSAF structure has an undesirable signal path delay caused by analysis and synthesis filters, which may lead to restrictive usage of the NSAF in real-time applications. To tackle the issue, two novel delayless structures (i.e., open-loop and closed-loop schemes) were proposed for the NSAF and they have been successfully applied in various real-time systems [21]. Recently, by associating the robust IWF-SSAF [18] with the delayless NSAF structures [21], the delayless IWF-SSAF algorithms [22] were presented to overcome both aforementioned difficulties and their efficacy was verified in several impulsive interference environments including active impulsive noise control (AINC) applications.

In this paper, we develop a block implementation of the delayless closed-loop IWF-SSAF algorithm [22], designed for the AINC systems. In the proposed algorithm, the block-processing with the overlap-save technique is employed to update the weight, which reduces the required computational complexity. Especially in the block-processing, multiple auxiliary past gradients are available for each subband, which leads to an opportunity to introduce an improved BDVSS algorithm (I-BDVSS) than the original BDVSS one [22], in terms of the averaged noise reduction (ANR) performance. The effectiveness of the proposed delayless block algorithm is validated using a symmetric alpha stable (SαS) distribution, whose real impulsive noise examples include heavy machinery in industrial setup, traffic noise, gun shot and explosion, noise in MRI room, and so on. Therefore, the proposed delayless block algorithm can be employed to reduce such various impulsive noises.

This paper is organized as follows: We first present a review of related work in the context of AINC in Section II. Then, the modified delayless closed-loop IWF-SSAF for the AINC is briefly introduced in Section III. In Section IV, its block implementation and improved BDVSS (I-BDVSS) algorithm are proposed along with the computational analysis. In Section V, several simulation results are provided under impulsive noise control environments to verify the convergence performance. Finally, concluding remarks are given in Section VI.

II. RELATED WORK

Several modified filtered-x least mean squares (FxLMS) algorithms have been presented for the AINC application. There are two main approaches. First, since the second order moment does not exist for the SαS distribution, the widely used FxLMS algorithm cannot give a stable convergence performance [23], [24]. Therefore, the problem of minimizing the lower fractional order moment $p < \alpha$ has been introduced for the AINC system to improve the robustness of the FxLMS, which results in filtered-x least mean p-power (FxLMP) algorithms [23]. Here, α controls the impulsive nature. Second, the peaky reference/error signals are truncated with a threshold value because the weight can be largely fluctuated by the peaky samples during the weight update due to the modelling error, which finally degrades the convergence performance [25]. However, the aforementioned two approaches should estimate the value of α or the reference/error signal statistic to determine the threshold value, which may not be available in practice.

Recently, the delayless IWF-SSAF algorithm with the BDVSS [22] was proposed for the AINC application. Unlike the aforementioned two approaches, the delayless IWF-SSAF was derived by adopting the robust ℓ_1-norm based optimization criterion. Furthermore, from the experiments performed in [22], the improved ANR performance was also obtained when compared with that of the above two conventional AINC approaches and their combinations. In this paper, the efficient implementation of the delayless IWF-SSAF [22] is developed by using the block-processing, which can be applied especially for small and low-cost devices such as earbuds.

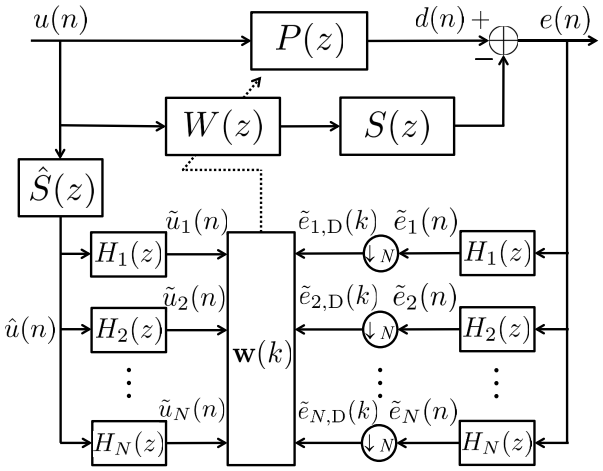

FIGURE 1. Delayless closed-loop IWF-SSAF structure modified for the AINC applications.

III. MODIFIED DELAYLESS CLOSED-LOOP IWF-SSAF FOR AINC APPLICATIONS

Fig. 1 illustrates the delayless closed-loop IWF-SSAF modified for the AINC systems [22]. The desired signal $d(n)$ is the output of the primary path $P(z)$ with the reference signal $u(n)$ as its input. In addition, N is number of subbands and k is a decimated sequence of n by a factor of N. Then, if $W(z)$ is modelled by a finite impulse response (FIR) filter $\mathbf{w}(k)$ of the length L, its output $y(n)$ can be written as $y(n) = \mathbf{w}^{\mathrm{T}}(k)\mathbf{u}(n)$ and error $e(n)$ can be expressed as follows:

$$e(n) = d(n) - s(n) * y(n), \tag{1}$$

where $\mathbf{u}(n) = [u(n), u(n-1), \ldots, u(n-L+1)]^{\mathrm{T}}$, $s(n)$ is the impulse response of the secondary path $S(z)$ with the length M, and $*$ denotes the linear convolution operation. The filtered-x signal $\hat{u}(n)$ is obtained by filtering $u(n)$ through the estimated secondary path $\hat{S}(z)$. Then, $\hat{u}(n)$ and $e(n)$ are split into subbands via the analysis filter $H_i(z)$, which leads to the subband signals, $\tilde{u}_i(n)$ and $\tilde{e}_i(n)$, respectively. The IWF-SSAF weight update [18] is given as

$$\mathbf{w}(k+1) = \mathbf{w}(k) + \mu \sum_{i=1}^{N} \frac{\tilde{\mathbf{u}}_i(k)\mathrm{sgn}(\tilde{e}_{i,\mathrm{D}}(k))}{\sqrt{\tilde{\mathbf{u}}_i^{\mathrm{T}}(k)\tilde{\mathbf{u}}_i(k) + \delta}}, \tag{2}$$

where μ is a step-size, $\tilde{\mathbf{u}}_i(k) = [\tilde{u}_i(kN), \ldots, \tilde{u}_i(kN-L+1)]^{\mathrm{T}}$, $\tilde{e}_{i,\mathrm{D}}(k)$ is a decimated sequence of $\tilde{e}_i(n)$ by a factor of N, and $\mathrm{sgn}(\cdot)$ represents the sign function.

IV. PROPOSED BLOCK IMPLEMENTATION WITH AN IMPROVED BDVSS

A. BLOCK IMPLEMENTATION OF MODIFIED DELAYLESS IWF-SSAF

Fig. 2 depicts a block implementation of Fig. 1. We employ a block-processing with an overlap-save method to update the weight. Here, the overlap rate is 0.5; thus, the weight is updated in every L fullband samples.

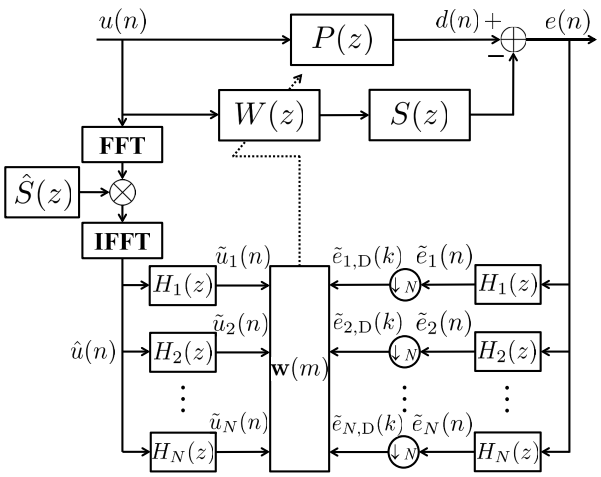

FIGURE 2. Proposed block implementation of the modified delayless closed-loop IWF-SSAF in Fig. 1.

Initially, the filtered-x signal $\hat{u}(n)$ is computed by using $2L$-point fast Fourier transform (FFT) as follows:

$$\hat{\mathbf{u}}^f(n) = \mathbf{u}^f(n) \odot \hat{s}^{\mathbf{f}}(n), \tag{3}$$

where $\odot$ represents the element-wise multiplication, $\hat{\mathbf{s}}^f(n) = \mathrm{FFT}\{\hat{s}(n)\}$, and

$$\mathbf{u}^f(n) = \mathrm{FFT}\{[u(n-2L+1), \ldots, u(n)]^{\mathrm{T}}\}. \tag{4}$$

Then, L new samples of $\hat{u}(n)$ are obtained by applying the inverse FFT to $\hat{\mathbf{u}}^f(n)$ and discarding first L samples. After that, $\tilde{u}_i(n)$ should be also computed in every L fullband samples due to the block processing of $\hat{u}(n)$ as follows:

$$\tilde{u}_i(n-l) = \mathbf{h}_i^{\mathrm{T}}\hat{\mathbf{u}}(n-l), \quad l = 0, \ldots, L-1, \tag{5}$$

where $\hat{\mathbf{u}}(n) = [\hat{u}(n), \hat{u}(n-1), \ldots, \hat{u}(n-Q+1)]^{\mathrm{T}}$, $\mathbf{h}_i$ is the coefficient vector of the impulse response of $H_i(z)$, and Q is the length of $\mathbf{h}_i$.

It should be stressed here that with the block processing, the weight of sign algorithms can be more efficiently updated in the time-domain rather than the frequency-domain. As shown in (2), the sign change of $\tilde{\mathbf{u}}_i(k)$ is only needed without any multiplications in the sign algorithms; on the other hand, the ℓ_2-norm based algorithms usually require the computation of the correlation between the input and error signals, and they can be more efficiently realized in the frequency-domain.

Accordingly, the proposed weight update scheme is efficiently implemented in the time-domain. Note that in (2), the weight update is carried out per N fullband samples. Therefore, there exist L/N number of the gradients in the block processing per L fullband samples. As a result, the proposed weight update scheme can be expressed as

$$\mathbf{w}(m+1) = \mathbf{w}(m) + \mu \sum_{i=1}^{N} \sum_{j=0}^{L/N-1} \frac{\tilde{\mathbf{u}}_i(k-j)\mathrm{sgn}(\tilde{e}_{i,\mathrm{D}}(k-j))}{\sqrt{\tilde{\mathbf{u}}_i^{\mathrm{T}}(k-j)\tilde{\mathbf{u}}_i(k-j)+\delta}}, \tag{6}$$

where m is a decimated sequence of n by a factor of L. As shown in (6), L/N number of gradients are given for each subband, which can be viewed as an averaged gradient and represent the true gradient more accurately [26]. The proposed delayless block IWF-SSAF algorithm is summarized in Algorithm 1.

Algorithm 1 Summary of the Proposed Block Implementation. $\mathbf{e}(k) = [e(kN), e(kN-1), \ldots, e(kN-Q+1)]^{\mathrm{T}}$

For $n = 0, 1, 2, \ldots,$
  $e(n) = d(n) - w^{\mathrm{T}}(m)\mathbf{u}(n)$
  For $k = 0, 1, 2, \ldots,$ where $kN = n$,
    $\tilde{e}_{i,\mathrm{D}}(k) = \mathbf{h}_i^{\mathrm{T}}\mathbf{e}(k), \quad i = 1, \ldots, N$
  End
  For $m = 0, 1, 2, \ldots,$ where $mL = n$,
    $\mathbf{u}^f(n) = \mathrm{FFT}\{[u(n-2L+1), \ldots, u(n)]^{\mathrm{T}}\}$
    $\hat{\mathbf{u}}^f(n) = \mathbf{u}^f(n) \odot \hat{\mathbf{s}}^f(n)$
    $[\hat{u}(n-L+1), \ldots, \hat{u}(n)]^{\mathrm{T}} = \mathrm{IFFT}\{\hat{\mathbf{u}}^f(n)\}(L+1:2L)$
    $\tilde{u}_i(n-l) = \mathbf{h}_i^{\mathrm{T}}\hat{\mathbf{u}}(n-l), \quad l = 0, \ldots, L-1$
  $\mathbf{w}(m+1) = \mathbf{w}(m) +$
    $\mu \sum_{i=1}^{N} \sum_{j=0}^{L/N-1} \frac{\tilde{\mathbf{u}}_i(k-j)\mathrm{sgn}(\tilde{e}_{i,\mathrm{D}}(k-j))}{\sqrt{\tilde{\mathbf{u}}_i^{\mathrm{T}}(k-j)\tilde{\mathbf{u}}_i(k-j)+\delta}}$
  End
End

B. IMPROVED BAND-DEPENDENT VARIABLE STEP-SIZE

An ℓ_1-norm based band-dependent variable step-size (BDVSS) algorithm [22] was introduced to improve the convergence of the original closed-loop IWF-SSAF. In this section, its improved BDVSS version (I-BDVSS) is proposed by exploiting the several past gradients for each subband, as shown in (6).

TABLE 1. Computational complexity of the proposed block implementation, in terms of number of real multiplications and additions per one fullband input sample.

Operations		Multiplications	Additions
Filtered-x	FFT, IFFT	$2 \times \frac{2\times 2L\log_2(2L)}{L} = 8\log_2(2L)$	$2 \times \frac{2\times 2L\log_2(2L)}{L} = 8\log_2(2L)$
	(3)	$\frac{4\times 2L}{L} = 8$	0
Subband signals	$\tilde{u}_i(n)$	$\frac{Q\times N\times L}{L} = Q\times N$	$\frac{(Q-1)\times N\times L}{L} = (Q-1)\times N$
	$\tilde{e}_{i,\mathrm{D}}(k)$	$\frac{Q\times L}{L} = Q$	$\frac{(Q-1)\times L}{L} = Q-1$
Weight update	(6)	$\frac{2\times L\times L}{L} = 2L$	$\frac{2\times (L-1)\times L}{L} = 2(L-1)$
I-BDVSS	$\mu^*_{i,j}(m)$	$N \times \frac{(L/N)}{L} = 1$	0
	time-average	$N \times \frac{(L/N)\times 2}{L} = 2$	$N \times \frac{(L/N)}{L} = 1$

The proposed I-BDVSS algorithm is derived by extending the ℓ_1-norm based minimization criterion [22], [27] to the multiple past gradients. Initially, the i-th subband *a posteriori* error $e_{i,p}(k-j)$ is defined as follows:

$$e_{i,p}(k-j) = d_{i,\mathrm{D}}(k-j) - \tilde{\mathbf{u}}_i^{\mathrm{T}}(k-j)\mathbf{w}_{i,j}(m+1) \quad (7)$$

$$\mathbf{w}_{i,j}(m+1) = \mathbf{w}(m) + \mu_i(m)\frac{\tilde{\mathbf{u}}_i(k-j)\mathrm{sgn}(e_{i,\mathrm{D}}(k-j))}{\sqrt{\tilde{\mathbf{u}}_i^{\mathrm{T}}(k-j)\tilde{\mathbf{u}}_i(k-j)+\delta}}, \quad (8)$$

where $d_{i,\mathrm{D}}(k)$, defined for the open-loop scheme, is obtained by filtering $d(n)$ through the analysis filter and further decimating it by a factor of N, $\mu_i(m)$ is an i-th band variable step-size, and $e_{i,\mathrm{D}}(k-j) = d_{i,\mathrm{D}}(k-j) - \tilde{\mathbf{u}}_i^{\mathrm{T}}(k-j)\mathbf{w}(m)$. In addition, (7) can be rewritten as follows:

$$e_{i,p}(k-j) = \tilde{e}_{i,\mathrm{D}}(k-j) - \mu_i(m)\, g_i(k-j), \quad (9)$$

$$g_i(k-j) = \frac{\tilde{\mathbf{u}}_i^{\mathrm{T}}(k-j)\tilde{\mathbf{u}}_i(k-j)\mathrm{sgn}(\tilde{e}_{i,\mathrm{D}}(k-j))}{\sqrt{\tilde{\mathbf{u}}_i^{\mathrm{T}}(k-j)\tilde{\mathbf{u}}_i(k-j)+\delta}}, \quad (10)$$

Note that in (9), $e_{i,\mathrm{D}}(k-j)$ is replaced with $\tilde{e}_{i,\mathrm{D}}(k-j)$ to suit the proposed closed-loop scheme [22].

Then, the I-BDVSS can be derived by minimizing the ℓ_1-norm of the *a posteriori* error as follows:

$$\mu^*_{i,j}(m) = \underset{\mu_i(m)}{\mathrm{argmin}} \ \|\tilde{e}_{i,\mathrm{D}}(k-j) - \mu_i(m)g_i(k-j)\|_1 \quad \text{subject to } \mu_{\mathrm{L}} \le \mu_i(m) \le \mu_{\mathrm{U}}, \quad (11)$$

where μ_{L} and μ_{U} are defined by the lower and upper bounds of the step-size, respectively. By observing that (11) is a piecewise linear convex problem as in [22], [27], its optimal solution $\mu^*_{i,j}(m)$ can be obtained by utilizing a similar numerical procedure to [22] as follows:

(i) $\mu^*_{i,j}(m) = \tilde{e}_{i,\mathrm{D}}(k-j)/g_i(k-j)$

(ii) $$\mu^*_{i,j}(m) = \begin{cases} \mu_{\mathrm{U}}, & \text{if } \mu^*_{i,j}(m) > \mu_{\mathrm{U}} \\ \mu_{\mathrm{L}}, & \text{if } \mu^*_{i,j}(m) < \mu_{\mathrm{L}} \\ \mu^*_{i,j}(m), & \text{otherwise.} \end{cases}$$

However, $\mu^*_{i,j}(m)$ may be increased due to the effect of the impulsive noise as discussed in [22], [27], which degrades the convergence. To prevent this possibility, the final step-size $\mu_i(m)$ is scheduled to be monotonically decreasing by merging L/N number of $\mu^*_{i,j}(m)$ for each subband as follows:

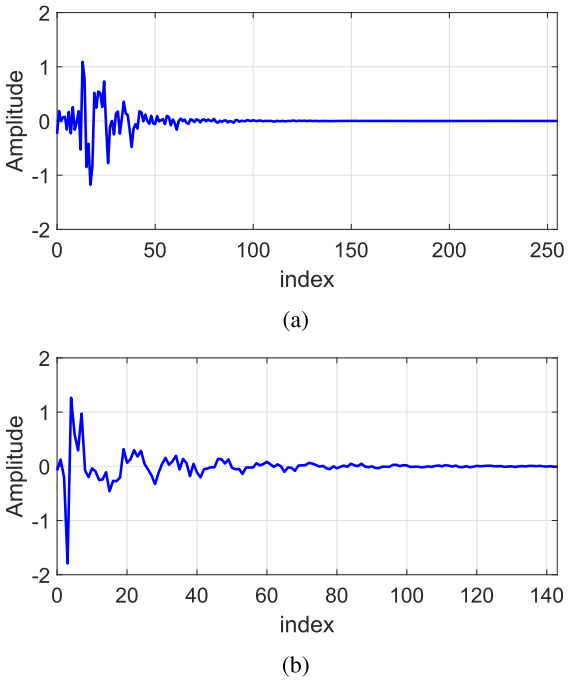

FIGURE 3. (a) Primary path and (b) secondary path used for the AINC system.

(i) $\mu_{i,0}(m-1) = \mu_i(m-1)$
$\mu_{i,j+1}(m-1) = \beta\mu_{i,j}(m-1) + (1-\beta)$

(ii) $\min\{\mu^*_{i,j}(m), \mu_{i,j}(m-1)\}, \quad j = 0, \ldots, L/N-1$

(iii) $\mu_i(m) = \mu_{i,L/N}(m-1)$,

where β is a smoothing parameter. When the proposed I-BDVSS $\mu_i(m)$ is combined with the proposed weight update (6) including the averaged gradient close to the true gradient, the proposed I-BDVSS algorithm can yield the enhanced convergence, which is demonstrated in the simulation results.

C. COMPUTATIONAL ANALYSIS

In Table 1, the computational cost of the proposed delayless block IWF-SSAF algorithm is analyzed in terms of number of real multiplications and additions per one fullband

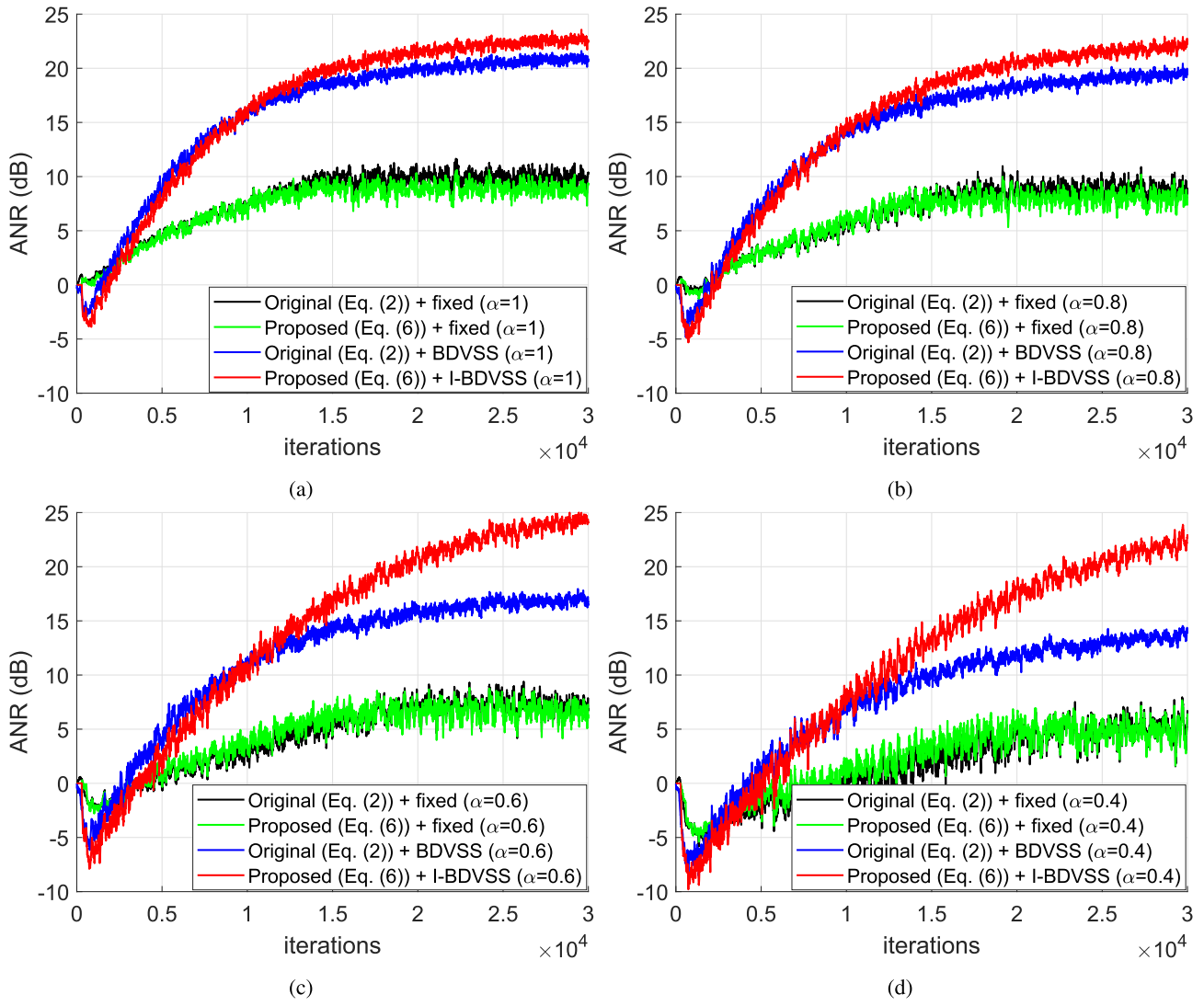

FIGURE 4. ANR performance obtained by the original delayless algorithm with the BDVSS [22] and the proposed delayless block algorithm with the I-BDVSS when (a) $\alpha = 1$, (b) $\alpha = 0.8$, (c) $\alpha = 0.6$, and (d) $\alpha = 0.4$.

TABLE 2. Computational complexity of the original delayless IWF-SSAF algorithm, in terms of number of real multiplications and additions per one fullband input sample.

Operations		Multiplications	Additions
Filtered-x	$\hat{u}(n)$	M	$M-1$
Subband signals	$\tilde{u}_i(n)$	$\frac{Q\times N\times N}{N} = Q\times N$	$\frac{(Q-1)\times N\times N}{N} = (Q-1)\times N$
	$\tilde{e}_{i,\mathrm{D}}(k)$	$\frac{Q\times N}{N} = Q$	$\frac{(Q-1)\times N}{N} = Q-1$
Weight update	(2)	$\frac{2\times N\times L}{N} = 2L$	$\frac{2\times (L-1)\times N}{N} = 2(L-1)$

input sample. In the proposed delayless algorithm, there are three main computational parts, i.e., (i) generating the filtered-x signal $\hat{u}(n)$, (ii) subband signals (i.e., $\tilde{u}_i(n)$ and $\tilde{e}_{i,\mathrm{D}}(k)$), and (iii) the weight update.

To generate $\hat{u}(n)$, the proposed algorithm demands $2L$-point FFT, its inverse FFT, and $2L$ complex multiplications for (3), which leads to $8\log_2(2L)+8$ multiplications and $8\log_2(2L)$ additions in total. In addition, QN multiplications and $(Q-1)N$ additions are required for $\tilde{u}_i(n)$, and Q multiplications and $(Q-1)$ additions are required for $\tilde{e}_{i,\mathrm{D}}(k)$. Also, the weight update needs $2L$ multiplications and $2(L-1)$ additions.

On the other hand, the original delayless algorithm demands the same computational burden as in the proposed delayless algorithm except generating the filtered-x signal $\hat{u}(n)$, as described in Table 2. The original algorithm should

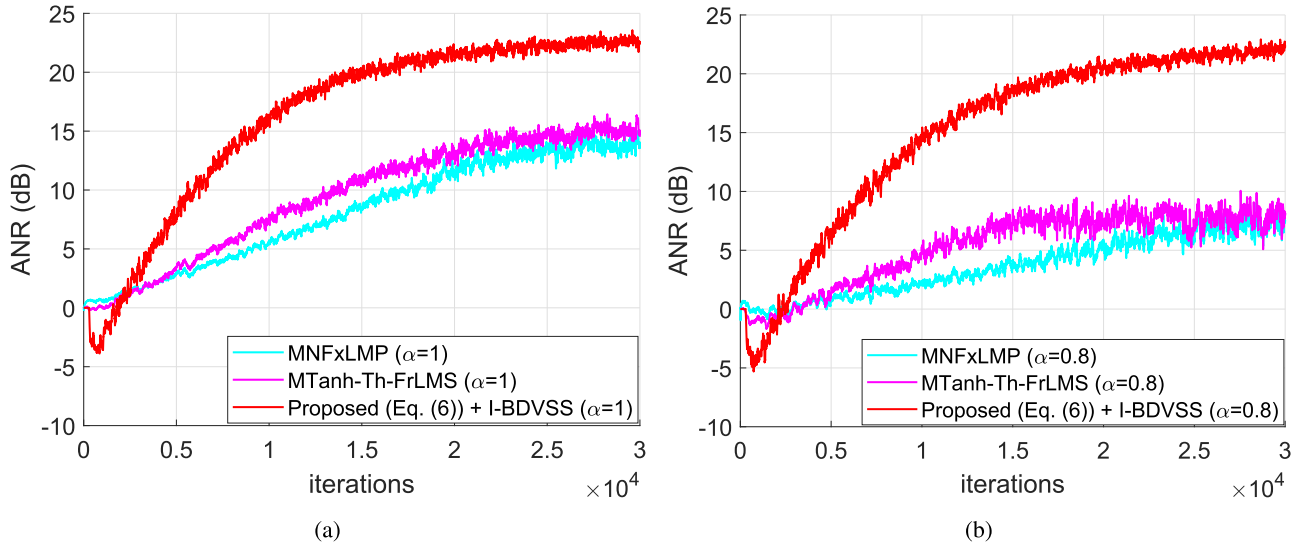

FIGURE 5. ANR performance obtained by the MNFxLMP [23] and the MTanh-Th-FrLMS [25] when (a) $\alpha = 1$ and (b) $\alpha = 0.8$.

require M multiplications and $(M-1)$ additions to compute $\hat{u}(n)$ since $\hat{u}(n)$ is directly filtered through the long fullband path $\hat{S}(z)$. Therefore, the proposed delayless algorithm can be more efficiently realized than the original delayless algorithm regardless of N since $M \gg 8\log_2(2L)+8$, e.g., $1024 \gg 8\log_2(2\times 2048)+8 = 104$ for $M = 1024$ and $L = 2048$ (when considering the number of multiplications only).

Furthermore, additional computational burden required by the proposed I-BDVSS algorithm is briefly analyzed in Table 1. Initially, $g_i(k-j) = \sqrt{\tilde{\mathbf{u}}_i^{\mathrm{T}}(k-j)\tilde{\mathbf{u}}_i(k-j)} \times \mathrm{sgn}(\tilde{e}_{i,\mathrm{D}}(k-j))$ can be computed without any further multiplications. Furthermore, as investigated in [13], $\mu_{i,j}^*(m)$ and the time-average scheme can be implemented with 1 and 2 multiplications, respectively. Therefore, the proposed I-BDVSS algorithm requires additional 3 multiplications in total, which is the same computational burden as required by the BDVSS [22].

V. EXPERIMENTS

In this section, the performance of the proposed delayless block IWF-SSAF algorithm was verified by simulations. In the simulations, similar settings as in [22] were used. Specifically, $u(n)$ was modelled as the SαS distribution with $\alpha = 0.4$–1. Its characteristic function can be expressed as

$$\phi(t) = e^{-\gamma|t|^{\alpha}}, \tag{12}$$

where γ is a dispersion parameter and $0 < \alpha < 2$ is the characteristic exponent. If $\gamma = 1$, the corresponding distribution is called *standard*. In the *standard* distribution, α controls the impulsive nature. That is, the lower α means the higher impulsive noise, and vice versa. $P(z)$ and $S(z)$ were respectively modelled as FIR filters with orders 512 and 192, as shown in Fig. 3 [28]. Note that $\hat{S}(z)$ was exactly the same as $S(z)$. $W(z)$ was modelled by an FIR filter of order 288. The averaged noise reduction (ANR) was adopted as a performance measure [22], which is defined as

$$\mathrm{ANR} = E\{\sigma_d(n)/\sigma_e(n)\}, \tag{13}$$

where

$$\sigma_d(n) = \lambda\sigma_d(n-1) + (1-\lambda)|d(n)| \tag{14}$$

$$\sigma_e(n) = \lambda\sigma_e(n-1) + (1-\lambda)|e(n)|. \tag{15}$$

For a fair comparison, the same optimally tuned parameters were used for the original BDVSS [22] and proposed I-BDVSS, as listed in Table 3.

TABLE 3. Parameters used in the simulations.

Algorithms	Parameters
Original [22], Proposed	$\mu = 0.01,\ \delta = 0.01,\ N = 8$
Original BDVSS [22], Proposed I-BDVSS	$\mu_i(0) = \mu_{\mathrm{U}} = 0.05,\ \mu_{\mathrm{L}} = 10^{-5},$ $\delta = 0.01,\ \beta = 1 - \frac{N}{2\cdot L},\ N = 8$

Fig. 4 shows the ANR performance of the original delayless algorithm with the BDVSS [22] and the proposed delayless block one with the I-BDVSS when $\alpha = 0.4$–1. For the fixed step-size scheme, both algorithms yielded almost the same ANR performance for all cases as expected (see green and black lines of Fig. 4). Note that smaller α means more severe impulsive noise control environment. Therefore, both algorithms experienced a gradual performance degradation as α is decreased. For the BDVSS scheme, the proposed I-BDVSS algorithm, even with less computational burden, achieved a better ANR performance in the steady-state for all considered α when compared with the original BDVSS algorithm (see blue and red lines of Fig. 4). Especially for smaller α, i.e., more severe impulsive noise control environment, the proposed I-BDVSS algorithm achieved higher performance gain over the original BDVSS [22].

In Fig. 5, the ANR performance of the proposed delayless block algorithm with the I-BDVSS was compared with that of

some conventional algorithms aimed at impulsive noise control when $\alpha = 0.8, 1$. The performance when $\alpha = 0.4, 0.6$ was not included in Fig. 5 since the conventional AINC algorithms exhibited unstable convergence performance. In the simulations, two existing AINC algorithms, i.e., modified normalized filtered-x least mean p-power (MNFxLMP) [23] and fractional FxLMS algorithm with a modified tanh threshold function (MTanh-Th-FrLMS) [25], were considered. In the MNFxLMP, the parameter p was set to $\alpha - 0.01$ as recommended. In the MTanh-Th-FrLMS, the fractional order was set to 0.65. Furthermore, in the modified tanh function, the thresholding parameters were determined by [1, 99] percentile of the reference signal and the tuning slope parameter was set to 2, as suggested. As a result, the MTanh-Th-FrLMS obtained a better ANR performance than the MNFxLMP for both cases. On the other hand, the proposed delayless block algorithm with the I-BDVSS yielded a superior ANR performance relative to the MTanh-Th-FrLMS.

VI. CONCLUSION

In this paper, a delayless closed-loop IWF-SSAF with an improved BDVSS (I-BDVSS) is designed for AINC systems, and its block implementation was developed. A computational complexity analysis was also performed, which reveals that the proposed delayless block IWF-SSAF algorithm is more efficiently implemented than the original delayless algorithm regardless of number of subbands. Finally, it was illustrated from the simulations that the proposed delayless algorithm with the I-BDVSS, requiring less computational complexity, can achieve the better ANR performance than the original delayless algorithm with the BDVSS. As a future work, we will consider the convergence analysis of the proposed delayless algorithm to investigate the effect of the averaged gradient under the AINC environment.

REFERENCES

[1] S. Haykin, *Adaptive Filter Theory*. London, U.K.: Pearson, 2014.
[2] P. S. R. Diniz, *Adaptive Filtering: Algorithms and Practical Implementation*. New York, NY, USA: Springer, 2008.
[3] Y. Yu, L. Lu, Z. Zheng, W. Wang, Y. Zakharov, and R. de Lamare, "DCD-based recursive adaptive algorithms robust against impulsive noise," *IEEE Trans. Circuits Syst. II, Exp. Briefs*, vol. 67, no. 7, pp. 1359–1363, Jul. 2020.
[4] S. Jiang and Y. Gu, "Block-sparsity-Induced adaptive filter for multi-clustering system identification," *IEEE Trans. Signal Process.*, vol. 63, no. 20, pp. 5318–5330, Oct. 2015.
[5] Y. Li, Z. Jiang, W. Shi, X. Han, and B. Chen, "Blocked maximum correntropy criterion algorithm for cluster-sparse system identifications," *IEEE Trans. Circuits Syst. II, Exp. Briefs*, vol. 66, no. 11, pp. 1915–1919, Nov. 2019.
[6] Y. Li, Z. Jiang, O. M. O. Osman, X. Han, and J. Yin, "Mixed norm constrained sparse APA algorithm for satellite and network echo channel estimation," *IEEE Access*, vol. 6, pp. 65901–65908, 2018.
[7] J. Liu and S. L. Grant, "Proportionate adaptive filtering for block-sparse system identification," *IEEE/ACM Trans. Audio, Speech, Language Process.*, vol. 24, no. 4, pp. 623–630, Apr. 2016.
[8] K. A. Lee, W. S. Gan, and S. M. Kuo, *Subband Adaptive Filtering: Theory and Implementation*. Hoboken, NJ, USA: Wiley, 2009.
[9] K. A. Lee and W. S. Gan, "Improving convergence of the NLMS algorithm using constrained subband updates," *IEEE Signal Process. Lett.*, vol. 11, no. 9, pp. 736–739, Sep. 2004.
[10] K. A. Lee and W. S. Gan, "Inherent decorrelating and least perturbation properties of the normalized subband adaptive filter," *IEEE Trans. Signal Process.*, vol. 54, no. 11, pp. 4475–4480, Nov. 2006.
[11] Z. Zheng and Z. Liu, "Influence of input noises on the mean-square performance of the normalized subband adaptive filter algorithm," *J. Franklin Inst.*, vol. 357, no. 2, pp. 1318–1330, Jan. 2020.
[12] J. Ni and F. Li, "Variable regularization parameter sign subband adaptive filter," *Electron. Lett.*, vol. 46, no. 24, pp. 1605–1607, Nov. 2010.
[13] J. H. Kim, J.-H. Chang, and S. W. Nam, "Sign subband adaptive filter with ℓ_1-norm minimisation-based variable step-size," *Electron. Lett.*, vol. 49, no. 21, pp. 1325–1326, Oct. 2013.
[14] J. Shin, J. Yoo, and P. Park, "Variable step-size sign subband adaptive filter," *IEEE Signal Process. Lett.*, vol. 20, no. 2, pp. 173–176, Feb. 2013.
[15] J. W. Yoo, J. W. Shin, and P. G. Park, "A band-dependent variable stepsize sign subband adaptive filter," *Signal Process.*, vol. 104, pp. 407–411, Feb. 2014.
[16] P. Wen and J. Zhang, "Robust variable step-size sign subband adaptive filter algorithm against impulsive noise," *Signal Process.*, vol. 139, pp. 110–115, Oct. 2017.
[17] J. Cho, H. J. Baek, B. Y. Park, and J. Shin, "Variable step-size sign subband adaptive filter with subband filter selection," *Signal Process.*, vol. 152, pp. 141–147, Nov. 2018.
[18] Y. Yu and H. Zhao, "Novel sign subband adaptive filter algorithms with individual weighting factors," *Signal Process.*, vol. 122, pp. 14–23, May 2016.
[19] Y. Yu, H. He, B. Chen, J. Li, Y. Zhang, and L. Lu, "M-estimate based normalized subband adaptive filter algorithm: Performance analysis and improvements," *IEEE/ACM Trans. Audio, Speech, Language Process.*, vol. 28, pp. 225–239, 2020.
[20] Z. Zheng, Z. Liu, and X. Lu, "Robust normalized subband adaptive filter algorithm against impulsive noises and noisy inputs," *J. Franklin Inst.*, vol. 357, no. 5, pp. 3113–3134, Mar. 2020.
[21] K.-A. Lee and W.-S. Gan, "On delayless architecture for the normalized subband adaptive filter," in *Proc. IEEE Multimedia Expo Int. Conf.*, Jul. 2007, pp. 1595–1598.
[22] J.-H. Kim, J. Kim, J. H. Jeon, and S. W. Nam, "Delayless individual-weighting-factors sign subband adaptive filter with band-dependent variable step-sizes," *IEEE/ACM Trans. Audio, Speech, Language Process.*, vol. 25, no. 7, pp. 1526–1534, Jul. 2017.
[23] M. T. Akhtar and W. Mitsuhashi, "Improving robustness of filtered-x least mean p-power algorithm for active attenuation of standard symmetric-α-stable impulsive noise," *Appl. Acoust.*, vol. 72, no. 9, pp. 688–694, Sep. 2011.
[24] Z. C. He, H. H. Ye, and E. Li, "An efficient algorithm for nonlinear active noise control of impulsive noise," *Appl. Acoust.*, vol. 148, pp. 366–374, May 2019.
[25] M. T. Akhtar, "An adaptive algorithm, based on modified tanh non-linearity and fractional processing, for impulsive active noise control systems," *J. Low Freq. Noise, Vibrat. Act. Control*, vol. 37, no. 3, pp. 495–508, Sep. 2018.
[26] J. J. Shynk, "Frequency-domain and multirate adaptive filtering," *IEEE Signal Process. Mag.*, vol. 9, no. 1, pp. 14–37, Jan. 1992.
[27] J. H. Kim, J.-H. Chang, and S. W. Nam, "Affine projection sign algorithm with ℓ_1 minimization-based variable step-size," *Signal Process.*, vol. 105, pp. 376–380, Dec. 2014.
[28] S. M. Kuo and D. R. Morgan, *Active Noise Control Systems: Algorithms and DSP Implementations*. Hoboken, NJ, USA: Wiley, 1996.

JUNG-HEE KIM (Member, IEEE) received the B.S., M.S., and Ph.D. degrees in electronic engineering from Hanyang University, Seoul, South Korea, in 2009, 2011, and 2016, respectively. From 2016 to 2019, he held a postdoctoral position with the Korea Institute of Science and Technology, Seoul, where he was involved in indoor positioning. Since 2019, he has been holding a postdoctoral position with the Research Institute of Electrical and Computer Engineering, Hanyang University, working on speech enhancement and acoustic echo cancellation. His research interests include adaptive signal processing, optimization, deep/machine learning, speech enhancement, speech processing, and acoustic signal processing.

JEONG-HWAN CHOI (Student Member, IEEE) received the B.S. and M.S. degrees in electronic engineering from Hanyang University, Seoul, South Korea, in 2017 and 2019, respectively, where he is currently pursuing the Ph.D. degree in electronics and computer engineering. His research interests include adaptive signal processing, speech signal processing, and speaker recognition.

SANG WON NAM (Senior Member, IEEE) received the B.S. degree in electrical engineering from Seoul National University, Seoul, South Korea, in 1981, and the M.S. and Ph.D. degrees in electrical engineering from The University of Texas, Austin, TX, USA, in 1987 and 1990, respectively. Since September 1991, he has been with the Department of Electronic Engineering, Hanyang University, Seoul, where he is currently a Professor. His research interests include digital signal processing, digital filter design, nonlinear signals and systems, multirate signal processing, active noise control, system identification, and biomedical engineering.

JOON-HYUK CHANG (Senior Member, IEEE) received the B.S. degree in electronics engineering from Kyungpook National University, Daegu, South Korea, in 1998, and the M.S. and Ph.D. degrees in electrical engineering from Seoul National University, South Korea, in 2000 and 2004, respectively. From 2000 to 2005, he was a CTO with Netdus Corporation, Seoul. From 2004 to 2005, he held a postdoctoral position with the University of California at Santa Barbara, Santa Barbara, where he was involved in adaptive signal processing and audio coding. He joined the Korea Institute of Science and Technology, Seoul, South Korea, as a Research Scientist, in 2005, where he was involved in speech recognition. From 2005 to 2011, he was an Assistant Professor with the School of Electronic Engineering, Inha University, Incheon, South Korea. He is currently a Full Professor with the School of Electronic Engineering, Hanyang University, Seoul. His research interests include speech recognition, deep/machine learning, artificial intelligence (AI), speech processing, acoustic signal processing, and bio-medical signal processing. He was a recipient of the IEEE/IEEK IT Young Engineer of the year 2011. He is also serving as an Editorial Board for *Digital Signal Processing* (Elsevier).